Metallogr. Microstruct. Anal. (2015) 4:467–474
DOI 10.1007/s13632-015-0231-3

TECHNICAL ARTICLE

Study of Coarsening in γ′ Precipitates by Diffusion Couples

C. G. Garay-Reyes[1] · S. E. Hernández-Martínez[2] · J. L. Hernández-Rivera[2] · I. Estrada-Guel[1] · H. J. Dorantes-Rosales[3] · J. J. Cruz-Rivera[2] · R. Martínez-Sánchez[1]

Received: 13 April 2015 / Revised: 18 September 2015 / Accepted: 21 September 2015 / Published online: 8 October 2015

Abstract The coarsening kinetics of γ' precipitates and Vickers hardness evolution are studied along a concentration gradient generated in a Ni-13.75Ti (at.%)/pure Ni diffusion couple at 1123, 1023, and 923 K. The formed concentration gradient allowed studying the aging process in Ni-rich Ni–Ti alloys with Ti content from 10.36 to 13.33 Ti (at.%). It was possible to determine experimentally the solvus line and precipitation boundary of the γ' phase at 1123 K by using the information obtained in such gradient. In addition to this, a comparison between the experimental coarsening kinetics and the LSW or TIDC theoretical models was carried out during the γ' precipitates coarsening.

Keywords Nickel-based alloys · Precipitation hardening · Coarsening · Diffusion couple · Vickers hardness · γ' Precipitates

This article is an invited paper selected from presentations at the 2014 Microscopy & Microanalysis Conference, held August 3–7, 2014, in Hartford, CT, USA, and has been expanded from the original presentation.

✉ C. G. Garay-Reyes
garay_820123@hotmail.com; carlos.garay@cimav.edu.mx

[1] Centro de Investigación de Materiales Avanzados (CIMAV), Laboratorio Nacional de Nanotecnología, Miguel de Cervantes 120, 311109 Chihuahua, Mexico

[2] Instituto de Metalurgia, Universidad Autónoma de San Luis Potosí, Sierra Leona 550, Col. Lomas 2a Sección, 78210 San Luis Potosí, Mexico

[3] Instituto Politécnico Nacional, ESIQIE-DIM, 118-556 Mexico, DF, Mexico

Introduction

The present work is based on the microstructural characterization method proposed by Miyazaki [1–7], the so-called Macroscopic Composition Gradient (MCG) method. This method enables determining solubility limits and precipitation boundaries as well as the evaluation of precipitates coarsening. It is based on the microstructural observation of a continuous concentration gradient, which can be generated by several methods, for instance, diffusion coupling, imperfect arc melting of sandwiched alloys, imperfect homogenization of coarse discontinuous precipitates, etc. [1–7]. On the other hand, many researchers, who used many different techniques [8–23], have studied the Ni-rich Ni–Ti system. The above-mentioned studies have concluded that cuboidal-type γ′ precipitates ($L1_2$ structure) aligned along ⟨100⟩ directions with faces parallel to {100} planes are the cause of hardening, but these precipitates coarsen at high temperatures and prolonged service times causing loss of coherency and eventually affect the mechanical properties.

Coarsening of precipitates is theoretically described in the model proposed by Lifshitz-Slyozov-Wagner (LSW theory) [24, 25], which predicts (for diffusion-controlled coarsening) precipitates dispersed in a fluid matrix (volume fraction of the precipitates (f_v) close to zero) that coarsen according to the following relationship:

$$r^3 = k_r t, \tag{1}$$

where r is the average precipitate radius, t is the aging time, and k_r is the coarsening rate constant. Some modifications exist in the LSW theory [26–33] that take into consideration the effect of f_v, $k_r = k_{r(f_v)}$. These theories differed to the LSW theory in a broader particle size distribution (*PSD*) and in an increase of k_r in function of increasing f_v.

However, a linear relationship between the cube of the average radius and aging time similar to LSW theory was evident. A different behavior of k_r during the coarsening has been reported in some Ni-based alloys, where k_r decreases in function of increasing f_v (at low volume fraction), which is known as anomalous coarsening [34–39]. Taking into consideration the anomalous coarsening and for avoiding the effect of f_v, a theory proposed by Ardell-Ozolins [40] and Ardell [41], the so-called trans-interface diffusion-controlled theory (TIDC) predicts a rate law given by the following:

$$\langle r\rangle^n \approx k_i t, \tag{2}$$

where r is the average precipitate radius, k_i is the coarsening rate constant, t is the aging time, and n is related to the width of the matrix/precipitate interphase [40, 41].

The main objectives of this investigation are to determine experimentally the solvus line and the precipitation boundary of γ' phase at 1123 K, study the coarsening of γ' precipitates at 1123, 1023, and 923 K, and evaluate the Vickers hardness of Ni-rich Ni–Ti alloys with different Ti concentrations using a single sample.

Experimental Procedure

Buttons of Ni–13.75Ti (at.%) alloy (C1) and Ni (C2) were melted in an electric-arc furnace under an argon atmosphere using pure Ni and Ti (99.99%). An assembly, which consists of the two specimens C1 and C2, was screwed to an austenitic stainless steel holder, which was encapsulated in a quartz tube and annealed at 1473 K for 28 h under an argon atmosphere to promote diffusion and generate a concentration gradient in the diffusion couple. Then the diffusion couple was encapsulated in a quartz tube to be solubilized at 1473 K for 2 h under an argon atmosphere followed by quenching in an ice-water mixture. Rectangular-shaped samples of around 2 mm in thickness were cut from the diffusion couple interface and aged isothermally at 1123, 1023, and 923 K during different times. Heat-treated samples were metallographically prepared, and then, they were electropolished at 223 K using an electrolyte solution of HNO_3/MeOH (30/70, volume ratio). The microstructural characterization was carried out using an Optical Microscopy (OM) and a Field-Emission Scanning Electron Microscopy (FE-SEM). Energy-Dispersive Spectroscopy (EDS) was used to determine variations in chemical composition along the concentration gradient. Finally, precipitates' size was measured from micrographs obtained by FE-SEM using commercial image analyzer software considering around 800 precipitates in each sample to obtain representative statistical values.

Results and Discussion

The diffusion process that occurs during annealing produces a characteristic microstructure in the diffusion couple where the Kirkendall effect and a mixture of phases are evidenced. Figure 1(a) shows the microstructure at the interface of the Ni–13.75Ti (at.%)/Ni diffusion couple after annealing at 1473 K. The variation of Ti concentration as a function of distance is also shown in this figure evidencing the concentration gradient at the diffusion couple interface. A region of about 140 μm that goes from the interface to the Ti-rich side, delimited by the solvus line, exhibits the presence of voids, which are formed due to the different diffusion rates of the diffusing elements (Kirkendall effect [42]). As reported elsewhere [42], the Ni diffusion rate is higher than that of Ti. Figure 1b and 1c show the solvus line and the precipitation boundary of the γ' phase, respectively, in thermal aged samples at 1123 K. In addition, η-$D0_{24}$ and γ' phases with plate-type and cuboidal-type morphology are identified in the sample. The solvus line and the precipitation boundary of the γ' phase experimentally determined by EDS were found at 9.16 and 9.92 Ti (at.%), respectively. These values are close to the corresponding values in the Ni–Ti phase diagram [21].

Five regions into the concentration gradient were studied (R1, R2, R3, R4, and R5) in order to make a comparison between regions of different chemical composition and f_v. These regions show different chemical composition and f_v (determined from the coherent solvus [43]) (see Table 1).

Figure 2 shows micrographs obtained by FE-SEM for R1, R2, R3, R4, and R5 regions after aging at 1023 K for 5000 min. γ' cuboidal-type precipitates with rounded corners aligned on the direction ⟨100⟩ of the matrix can be seen in these results. η plate-type precipitates, which grows in the (111) plane of the matrix phase was also observed.

Precipitate coarsening is especially important when aging treatment is considered to enhance the mechanical behavior of precipitation-hardened materials. At a particular aging temperature, precipitate size increases as a function of aging time. The strength of the alloy increases along with the precipitate size, reaches a maximum value and then decreases. The coarsening behavior of γ' precipitates can be quantified by determining the (i) average precipitate size, (ii) experimental precipitate size distributions (*PSD's*), and (iii) growth rate of precipitates. The equivalent radius is calculated and used as a size parameter to determine the experimental *PSD's*; the probability density, $\rho^2 f(\rho)$, is determined by the following equation [44]:

$$\rho^2 f(\rho) = \frac{N_i(r, r+\Delta r)}{\sum N_i(r, r+\Delta r)} \frac{\bar{r}}{\Delta r}, \tag{3}$$

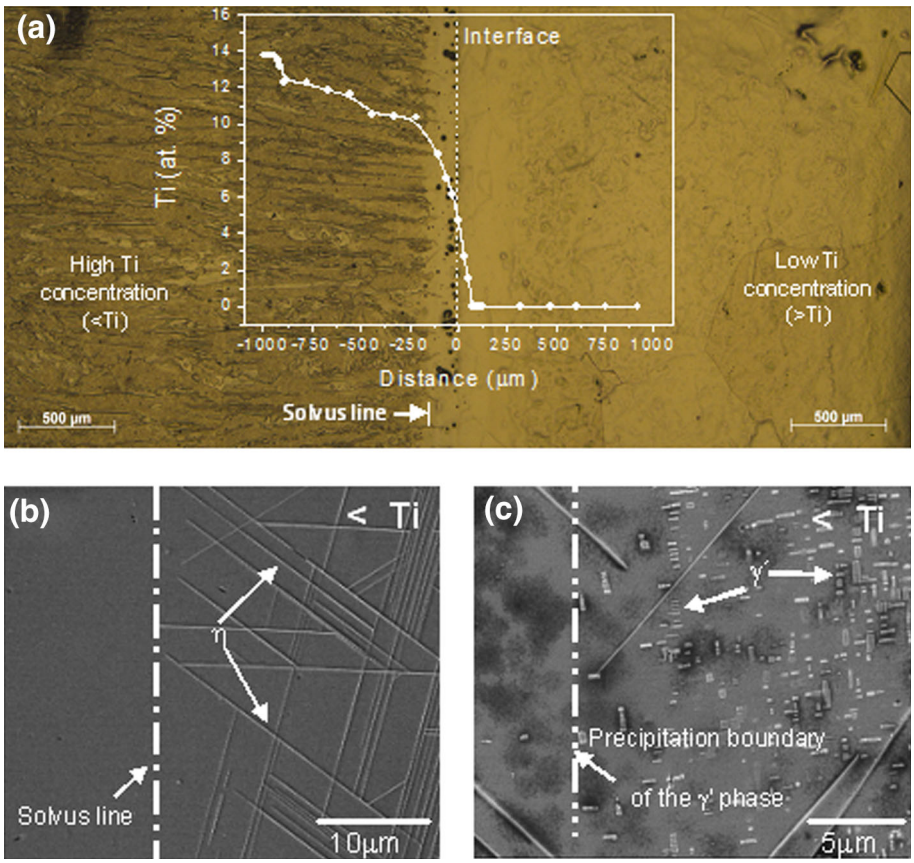

Fig. 1 (**a**) Optical micrograph of Ni–13.75 Ti (at.%)/Ni diffusion couple and Ti concentration profile after annealing at 1473 K, (**b**) and (**c**) FE-SEM images indicating the solvus line (*dashed dotted line*) and precipitation boundary of the γ' phase (*dashed double dotted line*) in samples thermal aged at 1123 K

Table 1 Chemical composition and f_v (determined from the coherent solvus [43]) in the five regions, R1, R2, R3, R4, and R5

Regions	Ti (at.%)	Volume fraction (f_v) %
R1	10.36 ± 0.28	5.8
R2	11.39 ± 0.14	21
R3	12.69 ± 0.19	43
R4	13.00 ± 0.22	47
R5	13.33 ± 0.28	52

where $\bar{r}$ is the average radius of the precipitates and $N_i(r, r + \Delta r)$ represents the number of precipitates in a given class interval Δr. The normalized radius (ρ) is defined as the ratio of $r/\bar{r}$. The LSW theory for diffusion-controlled coarsening leads to a highly asymmetric *PSD* with a cutoff near the particle radius ($\rho = 1$) and the *PSD's* for TICD are based entirely on the n parameter [45], $n = 2.281$ in rate law for Ni–Ti system [46]. Figure 3 shows a comparison between the experimental *PSD's* and the LSW, and TIDC theoretical distributions in R2 region aging at 1023 K for different times.

The probability density falls in the middle of the distribution ($\rho = 1$) in the histograms obtained for all temperatures; and then the extreme increases ($\rho = 0.8$ and 1.2) as a function of aging time making a broad distribution. This is due to that large precipitates grow at the expense of the dissolution of small precipitates. The experimental results show that there is not a perfect fit between the experimental PSD's and the two theoretical distributions. The experimental results best approach to the LSW theory in short aging times, while they fit better with the TIDC theory in long aging times.

The kinetics of precipitates growth during coarsening is expected to follow the next relationship:

$$r = k_r t^{1/m}, \tag{4}$$

where r is the average precipitate size, t is the aging time, k_r is a rate constant, and $1/m$ is the growth exponent. The values of the growth exponent for R1, R2, R3, R4, and R5 regions in the sample aged at 1023 K were obtained since the plot of ln r vs ln t, values obtained are shown in Table 2. The fit to the linear dependence is represented by the calculated linear regression coefficient, R^2. According to these results, it is evident that in R1 the value of the growth exponent ($1/m = 0.26$) was the highest among all the regions studied. As Ti content increases (from R1 to R5), the f_v of precipitates also increases and growth exponent values decrease to a value of $1/m = 0.13$. This

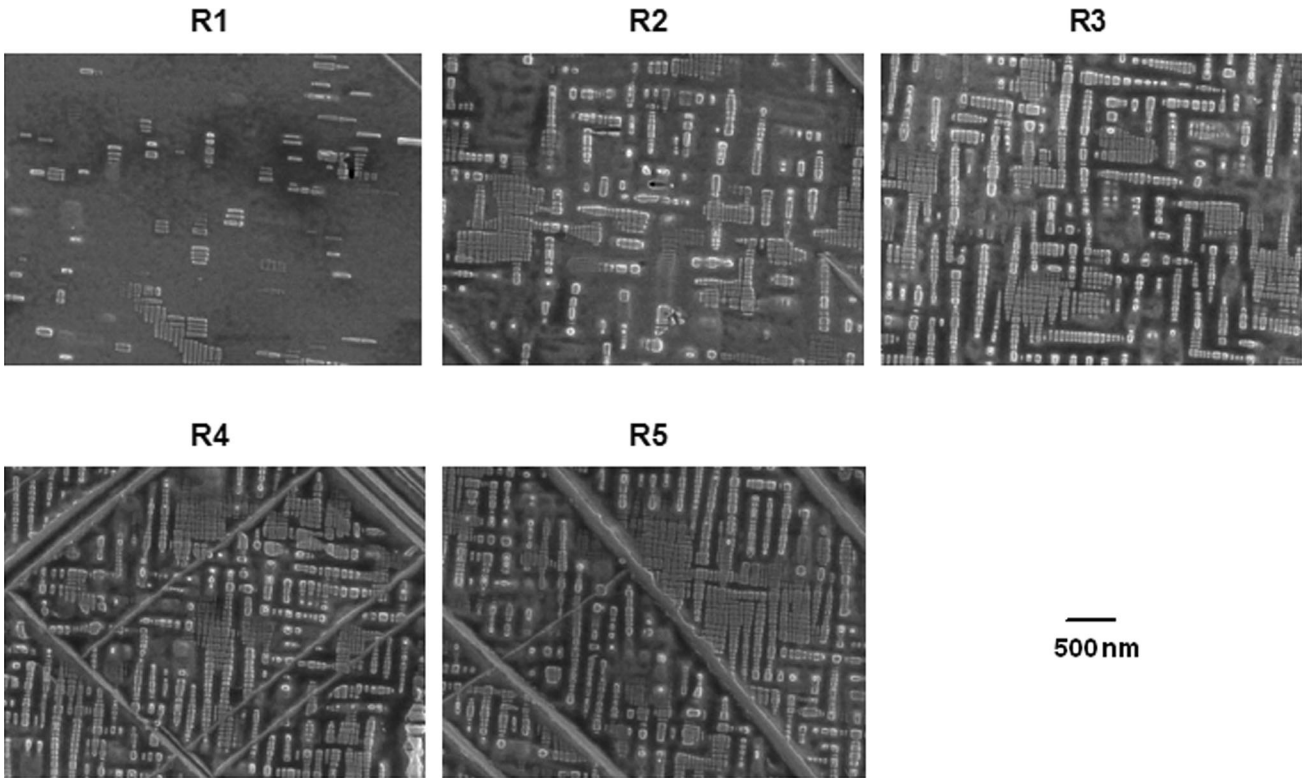

Fig. 2 FE-SEM micrographs of R1, R2, R3, R4, and R5 regions after aging at 1023 K for 5000 min

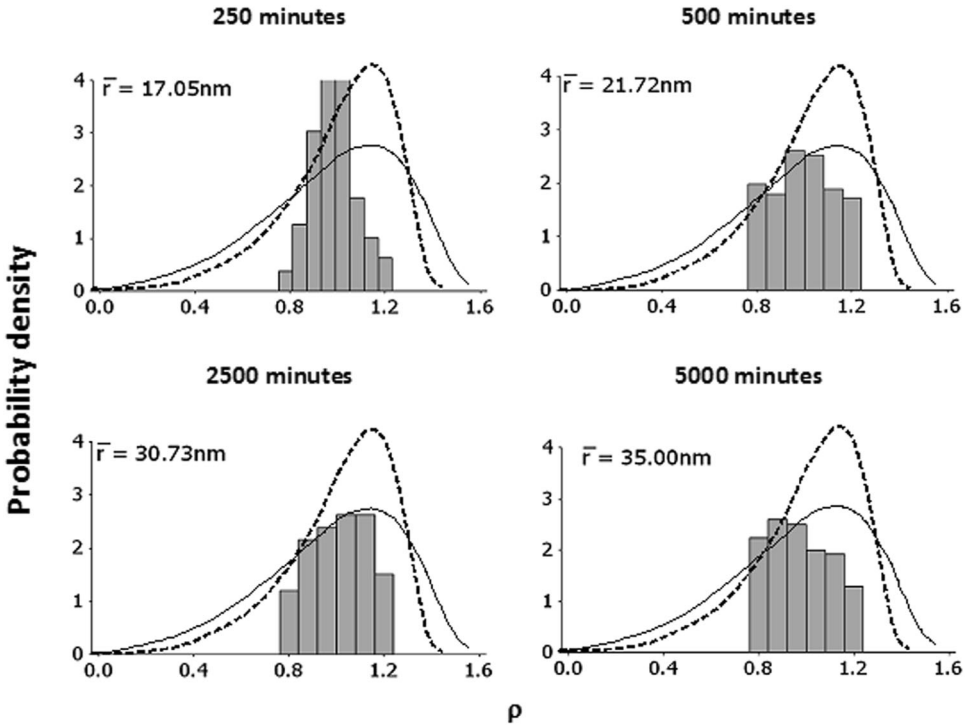

Fig. 3 Precipitate size distributions for R2 region after aging at 1023 K for different times (*dashed line* LSW and *straight line* TIDC distribution)

value is close to the value obtained by Sequeira et al. [44], ($1/m = 0.07$), during coarsening of γ' large precipitates in Ni–Al–Mo system with bimodal size distribution. These authors suggested that the elastic strain fields surrounding the matrix/precipitate interface were responsible for the relatively low coarsening kinetics.

Table 2 Values of the growth exponent for R1, R2, R3, R4, and R5 regions in the sample aged at 1023 K

Regions	$1/m$	R^2
R1	0.26	0.94542
R2	0.24	0.97542
R3	0.23	0.98241
R4	0.18	0.86537
R5	0.13	0.96346

Average precipitate size data were used to evaluate the approach to the rate law of the LSW and TIDC theories. Plots of "r^3 vs. t" and "$r^{2.281}$ vs. t" for R1, R2, R3, R4, and R5 regions in the sample aged at 1023 K are presented in Fig. 4. It can be seen that both r^3 and $r^{2.281}$ exhibit an approximately linear behavior with t. The fit to linear dependence is represented by the calculated linear regression coefficient, R^2. The coarsening rate constants (k_r and k_i) were calculated from the slope by linear regression analysis. The results showed that as f_v of the precipitates increases, the rate constants (k_r and k_i) decrease, which is contrary to the proposed modified LSW theory [47]. The above results suggested that the anomalous coarsening is present in this system for high f_v of precipitates. This kind of coarsening has been previously reported [35–39] in different Ni-base alloys. It is important to mention that in the region R4 different values are observed in comparison with the behavior of the other regions.

Figure 5 shows plots "r^3 vs. t" and "$r^{2.281}$ vs. t" for R4 region aged at 1123, 1023, and 923 K to evaluate the effect of temperature on coarsening rate constants (k_r and k_i). The coarsening rate constant (k_r and k_i) calculated shows a

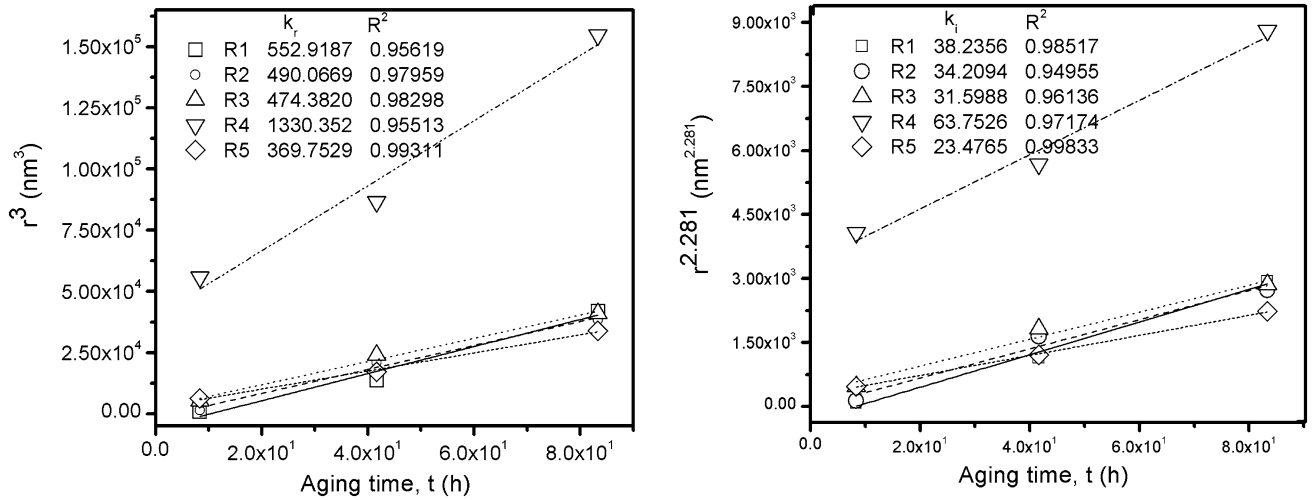

Fig. 4 Plots of r^3 vs. t (LSW theory) and $r^{2.281}$ vs. t (TIDC theory) for R1, R2, R3, R4, and R5 regions in the sample aged at 1023 K

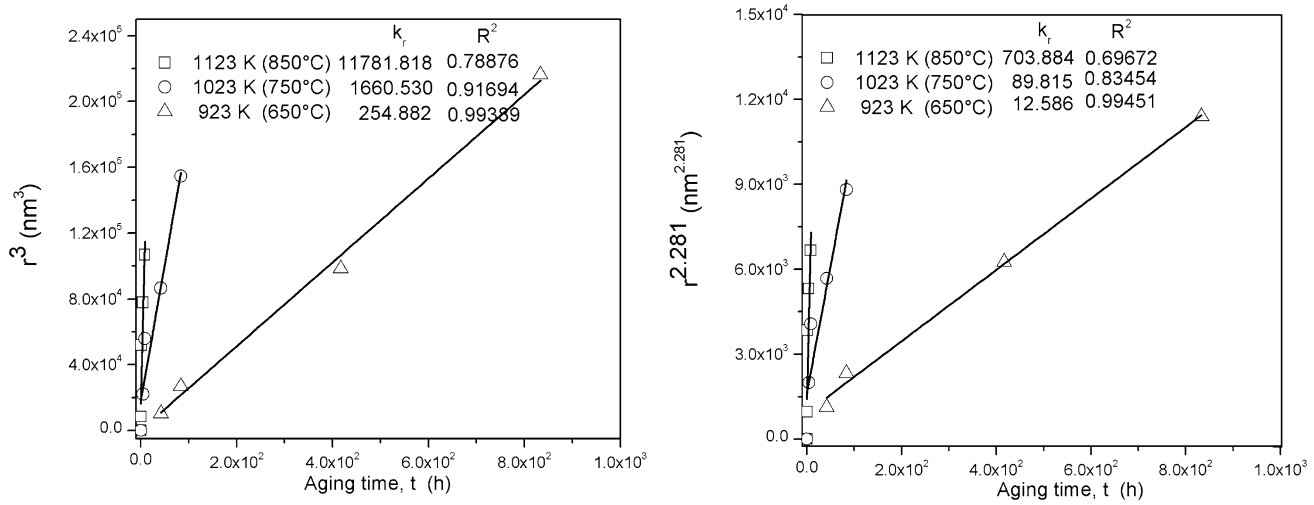

Fig. 5 Plots of r^3 vs. t (LSW theory) and $r^{2.281}$ vs. t (TIDC theory) for R4 region in the sample aged at 1123, 1023, and 923 K

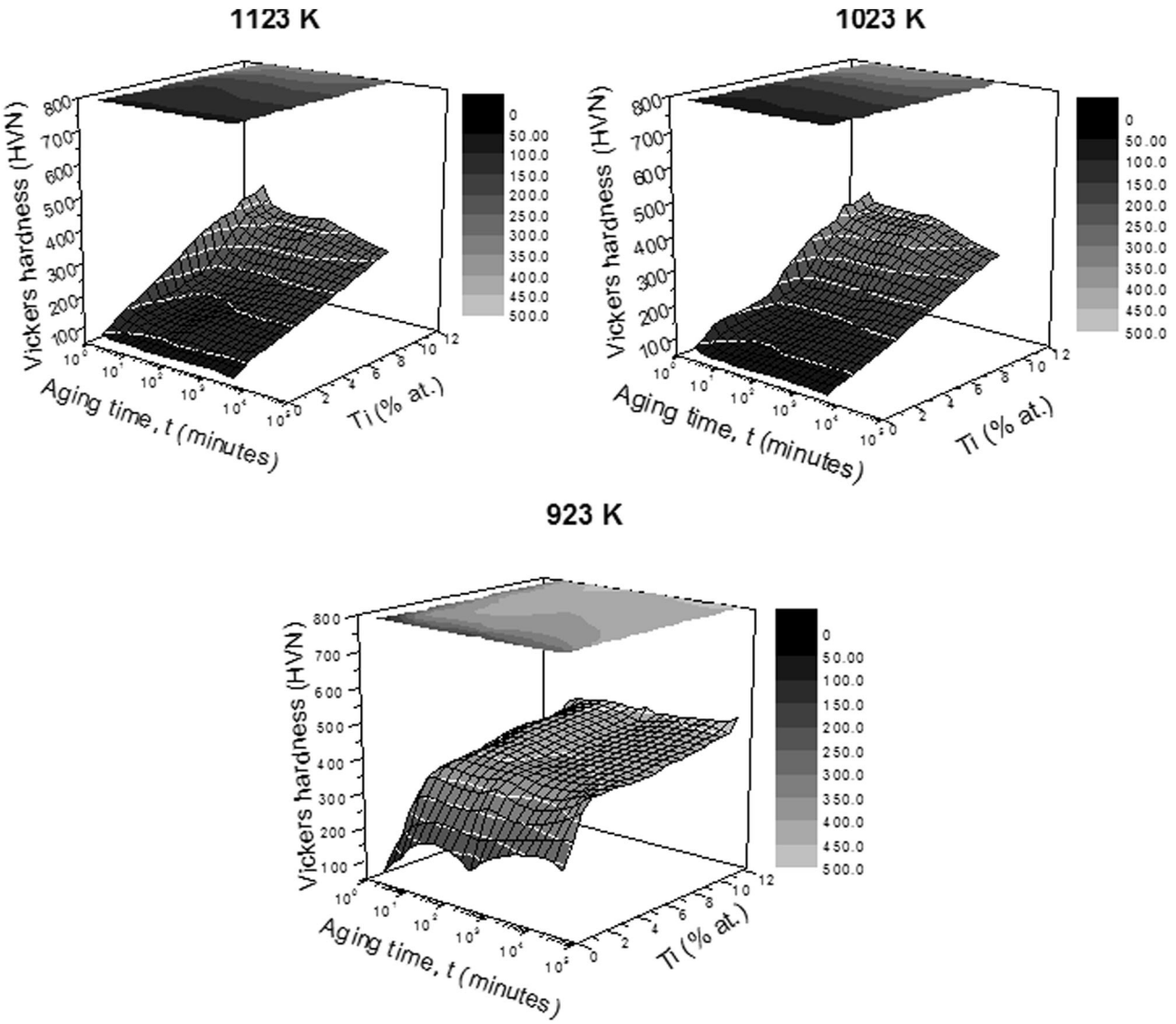

Fig. 6 Age-hardening curves obtained as a function of Ti concentration at 1123, 1023, and 923 K

strong temperature dependence as it can be seen in Fig. 5. The activation energy values obtained from the Arrhenius plot (ln k vs. $1/T$), for the TIDC (Q_i) and LSW (Q_r) theories, in R4 region are 164.5688 and 172.6173 kJ mol^{-1}.

The variation in Vickers hardness (HVN) as function of aging time in Ni-rich Ni–Ti alloys with different Ti concentrations aged at 1123, 1023, and 923 K is shown in Fig. 6. In general, the hardening effect is associated to the interaction between dislocations and the strain fields surrounding precipitates, and the softening effect is associated to coarsening and coherency loss of precipitates [48]. The maximum Vickers hardness observed for all temperatures is related with the presence of γ' precipitates. As the aging temperature decreases, f_v of precipitates and Vickers hardness increase but there is no precipitation hardening at concentrations less than 6Ti (at.%).

Conclusions

The use of a concentration gradient for the microstructural characterization of Ni-rich Ni–Ti alloys with different Ti concentrations allows determining phase boundaries, studying γ' precipitates coarsening with different f_v, and evaluation of mechanical properties by Vickers hardness measurements in a single sample. In addition, this method allows a comprehensive study of age-hardening curves in different alloys, being the limit the diffusion degree achieved in the concentration gradient. The solvus line and precipitation boundary of the γ' phase at 1123 K were experimentally determined in 9.16 and 9.92Ti (at.%), respectively. It was found that the experimental coarsening kinetics does not fit with the LSW and TIDC theoretical models during coarsening of γ' precipitates, but effects of

coalescence and elastic strains that influence the coarsening kinetics and that associated with f_v of precipitates are observed. The activation energy values for the LSW and TIDC theoretical models in R4 were 164.5688 and 172.6173 kJ mol^{-1}, respectively. Finally, the maximum Vickers hardness obtained in age-hardening curves at 1123, 1023, and 923 K of Ni-rich Ni–Ti alloys at different Ti concentrations was associated to the presence of γ' precipitates.

Acknowledgments The technical assistance of Wilber Antúnez Flores for FE-SEM characterization is greatly appreciated. The first author would like to thank CONACYT for the scholarship given and extends a special acknowledgement to the Instituto Politécnico Nacional (IPN) for the facilities provided for performing the experimental work.

References

1. T. Miyazaki, T. Koyama, S. Kobayashi, A new characterization method of the microstructure using the macroscopic composition gradient in alloys. Metall. Mater. Trans. **27A**, 949–954 (1996)
2. S. Kobayashi, T. Sumi, T. Koyama, T. Miyazaki, Determination of coherent phase boundaries in Ni-V and Ni-Mo alloys by utilizing macroscopic composition gradient. J. Jpn. Inst. Metals. **60**, 22–28 (1996)
3. T. Miyazaki, S. Kobayashi, T. Koyama, Determination of the critical nucleus size of precipitates using the macroscopic composition gradient method. Metall. Mater. Trans. **30A**, 2783–2789 (1999)
4. T. Miyazaki, A new evaluation method of phase decomposition by utilizing the macroscopic composition gradient in alloys, in *Proceedings of the International Conference on Solid-Solid Phase Transformation* (1999), pp. 15–22
5. T. Miyazaki, T. Kozakai, C.G. Schoen, Precipitate nucleation near the edge of miscibility gap, in *Proceedings of Solid-to-Solid Phase Transformation in Inorganic Materials* (2005), pp. 271–290
6. T. Miyazaki, S. Kobayashi, Evaluation of microstructures in alloys having a macroscopic composition gradient. Philos. Mag. **90**, 305–316 (2010)
7. T. Miyazaki, Development of 'Macroscopic Composition Gradient Method' and its application to the phase transformation. Prog. Mater Sci. **57**, 1010–1060 (2012)
8. A. Taylor, R.W. Floyd, The constitution of nickel-rich alloys of the Ni-Ti-Al system. J. Inst. Metals. **81**, 25–32 (1952–53).
9. Y.A. Bagariatskii, Y.D. Tiapkin, The mechanism of structure transformations in age hardening alloys based on nickel. Soviet Phys. Cryst. **2**, 414–421 (1957)
10. C. Bücle, B. Genty, J. Manenc, Quelques aspects de la precipitation dans un alliage nickel-titane. Rev. Metall. **56**, 247–259 (1959)
11. Y.A. Bagariatskii, Y.D. Tiapkin, The mechanism of structure transformations in age hardening alloys based on nickel. Soviet Phys. Cryst. **2**, 414–421 (1957)
12. D.H. BenIsrael, M.E. Fine, Precipitation studies in Ni-10 at% Ti. Acta Metall. **11**, 1051–1059 (1963)
13. S.L. Sass, T. Mur, J.B. Cohen, Diffraction contrast from non-spherical distortions in particular a cuboidal inclusion. Phil. Mag. **16**, 680–690 (1967)
14. K. Saito, R. Watanabe, Precipitation in Ni-12 at% alloy. Jpn. J. Appl. Phys. **83**, 14–23 (1969)
15. A.J. Ardell, The growth of gamma prime precipitates in aged Ni-Ti alloys. Metall. Trans. **1**, 525–534 (1970)
16. R. Sinclair, J.A. Leake, B. Ralph, On the determination of a local order parameter in a nickel-titanium alloy. Phys. Stat. Sol. A **26**, 285–298 (1974)
17. D.E. Laughlin, Spinodal decomposition in nickel based nickel-titanium alloys. Acta Metall. **24**, 53–58 (1976)
18. K. Hashimoto, T. Tsujimoto, X-ray diffraction patterns and microstructures of aged Ni-Ti alloys. Trans. JIM. **19**, 77–84 (1978)
19. R. Grune, Decomposition of Ni-12 at.% Ti by atom-probe field-ion microscopy. Acta Metall. **36**, 2797–2809 (1988)
20. A. Cerri, B. Schönfeld, G. Kostorz, Decomposition kinetics in Ni-Ti alloys. Phys. Rev. B. **42**, 958–960 (1990)
21. P. Vyskocil, J.S. Pedersen, G. Kostorz, B. Schönfeld, Small-angle neutron scattering of precipitates in Ni-rich Ni-Ti alloys-I. Metastable states in poly-and single crystal. Acta Mater. **45**, 3311–3318 (1997)
22. R. Bucher, B. Deme, H. Heinrich, J. Kohlbrecher, M. Kompatscher, G. Kostorz, J.M. Schneider, B. Schönfeld, M. Zolliker, In situ neutron scattering studies of order and decomposition in Ni-rich Ni-Ti. Mater. Sci. Eng. A **324**, 77–81 (2002)
23. M. Kompatscher, B. Schönfeld, H. Heinrich, G. Kostorz, Phase separation in Ni-rich Ni-Ti: the metastable states. Acta Mater. **51**, 165–175 (2003)
24. C. Wagner, Theorie der alterung von nierderschlägen durch umlösen. Z. Elektrochem. **65**, 581–591 (1961)
25. M. Lifshitz, V.V. Slyozov, The kinetics of precipitation from supersaturates solid solutions. J. Phys. Chem. Solids **19**, 35–50 (1961)
26. A.J. Ardell, The effect of volume fraction on particle coarsening: theoretical considerations. Acta Metall. **20**, 61–71 (1972)
27. D. Brailsford, P. Wynblatt, The dependence of Ostwald ripening kinetics on particle volume fraction. Acta Metall. **27**, 489–497 (1979)
28. C.K.L. Davies, P. Nash, R.N. Stevens, The effect of volume fraction of precipitate on Ostwald ripening. Acta Metall. **28**, 179–189 (1980)
29. K. Tsumaraya, Y. Miyata, Coarsening models incorporating both diffusion geometry and volume fraction of particles. Acta Metall. **31**, 437–452 (1983)
30. J.A. Marqusee, J. Ross, Kinetics of phase transitions: theory of Ostwald ripening. J. Chem. Phys. **80**, 536–543 (1984)
31. M. Tokuyama, K. Kawasaki, Statistical-mechanical theory of coarsening of spherical droplets. Phys. A **123**, 386–411 (1984)
32. P.W. Voorhees, M.E. Glicksman, Solution to the multiparticle diffusion problem with applications to Ostwald ripening—I. Theory. Acta Metall. **32**, 2001–2012 (1984)
33. P.W. Voorhees, M.E. Glicksman, Solution to the multiparticle diffusion problem with applications to Ostwald ripening—II. Computer simulations. Acta Metall. **32**, 2013–2030 (1984)
34. A.J. Ardell, Observations on the effect of volume fraction on the coarsening of γ′ precipitates in binary Ni-Al alloys. Scripta Metall. Mater. **24**, 343–346 (1990)
35. A. Maheshwari, A.J. Ardell, Anomalous coarsening behavior of small volume fractions of Ni_3Al precipitates in binary Ni-Al alloys. Acta Metall. Mater. **40**, 2661–2667 (1992)
36. J.H. Cho, A.J. Ardell, Coarsening of Ni_3Si precipitates at volume fractions from 0.03 to 0.30. Acta Mater. **46**, 5907–5916 (1998)
37. D.M. Kim, A.J. Ardell, The volume-fraction dependence of Ni_3Ti coarsening kinetics-new evidence of anomalous behavior. Scripta Mater. **43**, 381–384 (2000)
38. D.M. Kim, A.J. Ardell, Coarsening of Ni_3Ge in binary Ni–Ge alloys: microstructures and volume fraction dependence of kinetics. Acta Mater. **51**, 4073–4082 (2003)

39. D.M. Kim, A.J. Ardell, Coarsening behavior of Ni_3Ga precipitates in Ni-Ga alloys: dependence of microstructure and kinetics on volume fraction. Metall. Mater. Trans. A **35**, 3063–3069 (2004)
40. J. Ardell, V. Ozolins, Trans-interface diffusion-controlled coarsening. Nat. Mater. **4**, 309–316 (2005)
41. A.J. Ardell, Quantitative predictions of the trans-interface diffusion-controlled theory of particle coarsening. Acta Mater. **58**, 4325–4331 (2010)
42. S. Hinotani, Y. Ohmori, The microstructure of diffusion-bonded Ti/Ni interface. J. Jpn. Inst. Metals. **29**, 116–124 (1988)
43. P.K. Rastogi, A.J. Ardell, The Coherent Solubilities of γ' in Ni-Al. Ni-Si and Ni-Ti alloys. Acta Metall. **17**, 595–602 (1969)
44. A.D. Sequeira, H.A. Calderon, G. Kostorz, J.S. Pedersen, Bimodal size distribution of γ precipitates in Ni-Al-Mo-II transmission electron microscopy. Acta Metall. Mater. **43**, 3441–3445 (1995)
45. J. Ardell, D.M. Kim, V. Ozolins, Ripening of $L1_2$-Ni_3Ti precipitates in the framework of the trans-interface diffusion-controlled theory of particle coarsening. Z Metallkde. **97**, 295–302 (2006)
46. J. Ardell, A1-L12 interfacial free energies from data on coarsening in five binary Ni alloys, informed by thermodynamic phase diagram assessments. J. Mater. Sci. **46**, 4832–4849 (2011)
47. A. Baldan, Progress in Ostwald ripening theories and their applications to the γ′ precipitates in nickel-base superalloy part I Ostwald ripening theories. J. Mater. Sci. **37**, 2171–2202 (2002)
48. Z. Guo, W. Sha, Quantification of precipitation hardening and evolution of precipitates Mater. Trans. **43**, 1273–1282 (2002)